Complete ^{1}H, $^{13}C\{^{1}H\}$, and ^{31}P NMR Spectral Parameters of Some Pyrophosphates

Esa Haapaniemi
Department of Organic Chemistry, University of Jyväskylä, FIN-40500, Finland

Keywords

NMR, ^{1}H, $^{13}C\{^{1}H\}$, ^{31}P, Pyrophosphates, iterative spectral analysis, molecular modeling

ABSTRACT

The ^{1}H, $^{13}C\{^{1}H\}$, and ^{31}P NMR spectral parameters of some pyrophosphates were determined in $CDCl_3$. The most complicated ^{1}H spectrum can be solved fully only as $(A_3MN)R_6XX'R_6'(MNA_3)'$, where R_6 (= $-N(CH_3)_2$) is coupled only to phosphorus (X). Second order coupling between phosphorus was found and solved with iterative analysis. A signal shape of one of the carbon resonance cannot be explained only with couplings. Explanation for exceptional shape was searched from molecular modeling results.

This article has been accepted for publication and undergone full peer review but has not been through the copyediting, typesetting, pagination and proofreading process which may lead to differences between this version and the Version of Record. Please cite this article as doi: 10.1002/mrc.4590

INTRODUCION

Organophosphate compounds have been studied for long because of their biological[1] activity and potential industrial use. Pyrophosphates are very important in biochemistry[2]. Basic formula for pyrophosphate anion $P_2O_7^{4-}$ points out that there are possibilities for several high-energy phosphate bonds. Tetraethyl pyrophosphate (compound 5) was synthetized already in 1854[3] and later[4], it was found to be an effective insecticide. As such, it resembles phosphorus containing chemicals that have been banned[5] as Chemical Warfare (CW) agents. Compound **5** has been studied with NMR previously at 60 MHz and 100 MHz for ^{1}H and at ~25 MHz for ^{31}P frequencies[6].

Several powerful NMR methods in determination of the structures of organophosphorus compounds have been published[7,8,9]. In cases of decomposing compounds, the decomposition products can be used to identify the original chemicals. In CW (Chemical Warfare) studies analysis of decomposition products is safer than handling the actual agents. One of the decomposing routes of ^{31}P containing agents is oxidization, where the phosphorus containing compounds are forming pyrophosphates. The produced pyrophosphates are not stable in the environment but can be easily detected. Simulated spectra can also be used for identifying unknown chemicals from complicated matrices of non-purified samples[10]. This is a safe way to verify if some dangerous or even banned CW chemicals have been used.

COMPOUNDS UNDER INVESTIGATION

The pyrophosphates under current study are composed of similar substructures that can be identified and studied separately using NMR spectroscopy. Figure 1 illustrates the starting molecule (Tabun 1) for the subgroup analysis and four different pyrophosphates derived from it with atom numbering.

Compounds **2** and **4** have one chiral center (Figure 1) and consequently the ^{1}H NMR resonances of their R and S isomers are indistinguishable. Compound **3** has two chiral centers; the RR/SS and RS/SR stereoisomers are giving two different spectra, which can have overlapping resonances.

Compound **5** is an interesting case. Despite the achirality of the molecule, all ^{1}H, $^{13}C\{^{1}H\}$ and ^{31}P spectra are very complex due to the second order coupling with the phosphorus. As the magnetically nonequivalent ^{31}P nuclei are coupled to each other, the second order coupling comes visible through all the resonances. This renders structural elucidation more complicated and the full spectral analysis is necessary.

All of the compounds were modeled and their minimum energy conformations solved with semi-empirical PM3 method. The minimum energy conformations were used to evaluate the differences in the molecular conformations and as starting conformers for torsion energy calculations.

Torsional studies were done on each of the compounds over the P-O-P bridge. The energy level results reveal that the rotation is slightly hindered. Indeed, careful spectral analysis indicated that the rotation barriers are possible to be isolating some conformations. They can have divergent spectral parameters, which are not totally averaged in NMR timescale. Hydrogen bonds are also possible and present in particular conformations. Potential hydrogen bonds were confirmed with AbInitio calculations for the compound 2 (see Supporting information).

The ^{1}H and ^{13}C NMR coupling constants available through analysis of all compounds were further verified with using them in simulation of the ^{31}P NMR spectra. In cases of compounds **3** and **5** it was impossible to find a good fit between the simulated and experimental ^{1}H or $^{13}C\{^{1}H\}$ spectra unless the two-bond ^{31}P-^{31}P coupling was included in the simulation.

ANALYSIS

Most of the ^{1}H resonances can be analyzed and simulated with sub-spectral analysis. If there is some second order system inside the structure, it can be used as part of each sub-system where the coupling has effect on the signal shape and on the combination lines. In the current analysis some of the molecules have two phosphorus nuclei that are coupled to each other with second order coupling. As phosphorus is a 100 % natural abundance spin ½ nucleus, the second order coupling has effect on the proton signals as well.

As Tabun (1) is previously known and NMR data has been published[11], it was used only as a starting point in the analysis of the pyrophosphates. All NMR parameters needed to be optimized for the full spectral analysis of the compounds **2-5**.

All ^{1}H resonances are visible and identifiable based on subgroup analysis of the measured spectra. Spectral fine structures of compounds **2-5**, however, are more complicated due to couplings over the entire molecule.

Identification of separate P^{i} and P^{ii} phosphorus resonances in the ^{31}P NMR spectrum of compounds **2** and **4** can be made based on their couplings to protons. Also the two bond coupling constants between phosphorus nuclei can be measured from one dimensional $^{31}P\{^{1}H\}$ spectrum yielding 17.9 Hz for both compounds. Similar value can be used as a starting value for simulating the ^{1}H- and $^{13}C\{^{1}H\}$ spectra of compounds **3** and **5**. Both have second order ^{31}P-^{31}P geminal J-coupling, which effects the ^{1}H and $^{13}C\{^{1}H\}$ resonance shapes.

Each proton is coupled to the proximal phosphorus. Neither coupling between protons flanking the P-O-P bridge nor ^{1}H-^{31}P coupling to distal phosphorus was observed. Only the second order coupling between the phosphorus nuclei had an effect on the ^{1}H-^{31}P and the $^{13}C^{31}P$ couplings.

Each compound and spectrum is analyzed separately. This procedure is described in detail in the following.

Analysis of compound **2**

The ^{1}H resonances can be identified easily based on the coupling patterns. ^{1}H resonances of the methyl groups bound to the nitrogen can be identified based on only one large coupling to the nearby phosphorus. The coupling between **N**-methyl protons and phosphorus is about 10.9 or 10.6 Hz, respectively. One dimethyl group is less shielded whereas the other two are more shielded. This information is in accordance with the molecular modelling results, where the two nitrogen bound dimethyl groups are in more crowded surroundings than the single dimethyl group near to O-ethyl group.

All ^{1}H chemical shifts and coupling constants of compound **1** (Tabun, see Ref 1.) were used as starting values in iterative analysis of compound **2**. The iterative analysis was quick and the final parameters did not significantly deviate from the input values. The iterated parameters are presented in Table 1. The simulated ^{1}H resonances show good correlation with the experimental data (Figure 2, after Table 1).

Assignment of the ^{13}C resonances is also based on the chemical shift differences. The *N*-methyl carbons all resonate at around 36 ppm. One of them is less shielded by chemical shift and has larger coupling to phosphorus, thus suggesting it to belong to the chiral P^{i}. The ethyl carbon close to the oxygen and methyl carbon at the end of the carbon chain are resonating at around their correlation table areas, and finalizing the identification.

C-a signal possesses unexpected features. The signal shape is more complicated than just a doublet. When the measured FID was apodized with a Gaussian windowing before Fourier transformation, there were six different peaks in two pairs for C-a resonance. All of them had

different intensities. The difference between the pairs was equal to the visible coupling constant to the nearby phosphorus. The visible intensity difference did however not fit to the idea about one more coupling.

Because of the complicated signal shape compound **2** was modelled with PM3 method and the torsion energy barriers calculated over the P-O-P bridge. The tension energy in some angles was so large that it forced the other bond to rotate towards minimum energy. That calculation did not cover all the angles. So the other torsion had to be locked in a constant position while the other was rotated and the energy of the system calculated. The results are shown in Figure 4.

As can be seen from the torsional energy map, the rotation energy barriers (over 30 kJ/mol with PM3 and around 200 kJ/mol with MM2) are enough to hinder the rotation. It could be possible that there are several rotational isomers overlapping, and the extra small peaks on the C-a resonance are explained by the amount of isomers in each stable energy level. This explanation would require confirmation by further measurements, for example in different temperatures. Such were not carried out for this study, which focuses on primary analysis of these compounds.

Additional H-bond interactions were modeled as well with setting the molecule in a predefined conformation and adding possible H-bonds to the structure minimized with AbInitio HF-611 MP structure minimizing calculations. Several stable conformers were found where the distance between methyl/methylene proton and some of the oxygens was

shorter than 2.6 Å (see Supporting information). This could allow hydrogen bonding to be conceivable; however no results from these calculations are presented here. One reason for indecisive results was varying geminal P-O-P angle (calculated values between 95-180°) as well as the twisting of amide bond[12].

No population estimations were made to the conformers, and further calculations possibly together with more measurements are needed to verify whether the H-bonds influence on splitting of the signal C-a. No other carbon resonances of the compound 2 show similar extra splitting.

All ^{13}C spectral parameters were calculated iteratively and are shown on Table 1. The final simulated resonances are presented in Figure 2 (after Table 1).

The two phosphorus nuclei are differently shielded, as manifested to separate signals in the $^{31}P\{^{1}H\}$ as well as normal ^{31}P NMR spectra. The geminal coupling 17.9 Hz was observed in the $^{31}P\{^{1}H\}$ spectrum. Although contribution of this coupling did not show noticeable effect on simulated ^{1}H spectrum, it was included in all of the calculations.

Based on the analysis of the ^{31}P spectra of compounds **3**, **4**, and **5** the chemical shifts of P^{i} and P^{ii} in compound **2** are 1.03 and 10.97 ppm, respectively. The spectral parameters from ^{1}H analysis were incorporated into the simulation of the ^{31}P resonances. The results confirmed that the resonance identification and the initial analysis of coupling constants were correct. The simulated ^{31}P NMR spectrum is shown together with the experimental data in Figure 2 (after Table 1).

Analysis of compound **3**

Compound **3** has two chiral centers and thus four isomers. Both of the stereo-isomeric pairs are giving their own signals to the ^{1}H, $^{13}C\{^{1}H\}$, and ^{31}P spectra. Especially the ^{1}H spectrum has several overlapping signals.

Expansions of the ^{1}H spectrum of compound **3** reveal that the spin-system is more complicated and cannot be analyzed with sub-spectral analysis. The signal pattern of ethylene protons between 4.0-4.2 ppm consists of four overlapping resonances, which are coupled to each other in pairs. In addition, the geminal coupling between the H-a protons is of the second order in both cases.

The ^{1}H resonances of compound **3** required simulation of both isomers at the same time. This demands the spectrum to be analyzed as two overlapping $(A_3MN)R_6XX'R_6'(MNA_3)'$ spin systems. R6 means the two nitrogen-connected methylene proton resonances and X is the second order coupled phosphorus.

Given that ^{1}H spectrum of compound **3** is quite complex and the signals from the isomeric pairs are severely overlapping, the optimization of the ^{1}H spectral parameters was first made on the basis of $^{1}H\text{-}\{^{31}P\}$ spectrum. The signal intensities provided information on the isomeric populations enabling the connection of resonances to the corresponding isomer. The isomer pairs were marked with low- and high field chemical shifts.

After adding $^{1}H\text{-}^{31}P$ couplings to the solved calculations, resonances of the H-a protons from both isomers could be solved iteratively, and the fit was seemingly correct. Total line-shape

analysis improved accuracy of the coupling constants between H-a and H-a' as well as between H-a/H-a' and H-b's. The coupling between the phosphorus was solved from the ^{1}H resonance iteration to be 18.1 Hz.

Fitting of the H-c was less straightforward. Even when the coupling between phosphorus nuclei and all the couplings within the molecule were taken into account, the calculated signals did not fit perfectly to the measured resonance. The rationale behind this discrepancy could be the rotational isomers contributing to resonance line-shapes inside the peak patterns and coming visible in NMR timescale. Also the nearby nitrogen is having additional effect on methyl protons resonances. The rotation was modelled around the P-O-P bridge similar to compound **2**.

The energy barriers on both cases were smaller (20 kJ/mol vs. 30 kJ/mol) for compound **3** than they were for compound **2** (Figure 4). Moreover, compound **3** is more stable based on the calculated energy (see Supporting information). As the energy barriers are not separating the conformers, the spectrum is averaged in NMR timescale and data can be solved.

The parameters from the best fit are shown in Table 1 and the resonance signals between measured and simulated spectra in Figure 5.

The carbon resonances in the $^{13}C\{^{1}H\}$ spectrum suggest coupling to two phosphorus nuclei, although the resonances are not doublets of doublets. The coupling routes to two separate phosphorus nuclei are different in length, i.e., the coupling constant is not the same, and coupling patterns does not fit to the measured. There are also additional small combination

lines visible in the spectrum stemming from the second order system between the phosphorus nuclei.

As the samples were not ^{13}C enriched, the possibility for two ^{13}C nuclei being close to one another is small, and the coupling between the ^{13}C nuclei can be omitted. Each of the ^{13}C resonances stems from a C-P-P system, where the ^{31}P is parts of a second order spin system. The coupling constant between magnetically non-identical phosphorus nuclei was first estimated to be the same as with compounds **2** and **4**, where it was measured to be 17.9 Hz.

The resonances could be simulated quite quickly as isolated second order systems, where each carbon is coupled to only one of the phosphorus. The second order coupling between the phosphorus nuclei is important, and the simulated $^{13}C\{^{1}H\}$ resonances resemble the experimental data only if the coupling between the phosphorus nuclei is larger than $\pm$16.5 Hz. The coupling constant between the phosphorus nuclei found from the iterative analysis of the ^{1}H spectrum (18.1 Hz) gives a good fit for all carbon resonances. Population difference between isomers can be deduced from the signal intensities and was given an estimation presented in Table 1. The solved parameters are presented in Table 1. The calculated $^{13}C\{^{1}H\}$ resonances compared with experimental ones are shown in Figure 5.

After the best possible iterated chemical shifts and coupling constants for ^{1}H data were found, the parameters were used for simulating the ^{31}P resonances. ^{31}P chemical shifts between diastereomers are unequal and give two separate but close signals in the spectrum. Within one conformation, for one, the resonances are indistinguishable. Comparison between simulated and experimental data is shown in Figure 5. The population differences were not taken into

account in the simulation of phosphorus resonances and the linewidth used in calculation was same for both isomeric pairs.

Analysis of compound **4**

Some signals of impurities are present under the signals of H-a, H-c, and H-d. That makes the iterative analysis more time-consuming. Fortunately the ^{1}H-{^{31}P} spectrum was also measured, and the ^{1}H parameters without ^{31}P couplings could be analyzed first. After solving the chemical shifts and the coupling constants they were copied to the analysis of the phosphorus coupled ^{1}H spectrum. When the copied parameters were kept locked, and only the coupling constants between phosphorus and each proton coupled to phosphorus were varied, the impurity signals could be identified and marked to be left out from the iterative line-shape analysis. After the line shape analysis the ^{1}H spectral parameters were accurate, and the locking of the chemical shifts and coupling constants could be removed. Final parameters were then solved iteratively. The results are presented in Table 1, and simulated spectral resonances compared to the measured ones are shown in Figure 6.

Torsional energy map over P-O-P bridge was calculated with PM3 method for compound **4**. There are similarities between the energy map in Figure 4 (see Supporting information). The barrier tops are around the same torsion angles, but the energy barrier over the rotation is in the case of compound **4** ca. 20 kJ/mol, when in compound **3** the energy barrier was around 25 kJ/mol and in compound **2** around 30 kJ/mol. The calculated energy level is also lower in the case of compound **4**, -1670 kJ/mol compared to -1430 kJ/mol (compound **3**) and -1190 kJ/mol (compound **2**).

The $^{13}C\{^{1}H\}$ spectral resonances resemble normal doublets due to coupling to single ^{31}P. On the measured spectrum there is one visible impurity peak, but it is not interfering with the analysis. The resonances of carbons C-c and C-d are close to each other making the two doublets to look like a triplet. Also the three methyl resonances C-b, C-d, and C-f are overlapping, but they can be analyzed with PERCH total line shape routines. Each carbon resonance can be analyzed separately as a sub-spectral part, but they were calculated and simulated together to make the signal intensities comparable. The results are presented in Table 1 and Figure 6.

The two doublets in the $^{31}P\{^{1}H\}$ spectrum ca. 18 ppm apart correspond to the two phosphorus nuclei. The 17.9 Hz coupling between them is first order, and it does not have any effect on the other couplings inside the molecule.

The phosphorus resonances were simulated with the chemical shifts observed in the ^{1}H decoupled phosphorus spectrum and the coupling constants obtained from the ^{1}H iterative analysis results. The simulated ^{31}P resonances, P^{i} and P^{ii}, were calculated with different linewidths, 3.0 Hz and 0.5 Hz, respectively owing to nitrogen nucleus close to P^{i}. Both of the used linewidths are marked on the comments in Figure 6.

Analysis of compound **5**

In the symmetric cases of compounds **3** and **5** the phosphorus nuclei are chemically but not magnetically equivalent. In the case of compound **5** the second order *J*-coupling between the phosphorus nuclei has an additional effect on the ^{1}H and ^{13}C NMR spectra, explaining e.g. the triplet like resonance in the $^{13}C\{^{1}H\}$ spectrum.

Due to strong coupling between the phosphorus nuclei and the close proximity of protons, the ^{31}P-nuclei are coupled to each nearby proton and carbon in the structure. The second order effects between ^{31}P and ^{1}H contribute to other couplings and the signal shape becomes more complicated.

The simulated spectrum does not resemble the measured spectrum if only sub-spectral simulation is done. Good fit of simulated signal shapes was obtained only after including the complete ^{1}H system and two ^{31}P nuclei into calculations. The full ^{1}H spectrum is a result of $(AA'E_3M_6)_2XX'(N_6P_3ZZ')_2$ spin-system, where X and X' are the second order phosphorus parts. The results are presented in Table 1 and Figure 7.

Using of the $(AA'E_3M_6)_2XX'(N_6P_3ZZ')_2$ spin-system resulted in a good fit except for the *N*-dimethyl resonances. For this part the measured combination lines and the signals between the main peaks are wider than in the simulation. This discrepancy may stem either from the $^{14}N/^{15}N$ coupling to the protons or from the small variation between parameters due to rotational isomers. Despite this small inconsistency the rotational energies were calculated for this compound as well (see Supporting information). Energy levels of the compound **5** are the smallest, meaning that compound **5** is the most stable structure of the four compounds

under study. Also the rotation barriers are smaller than with the other compounds. It can be estimated, that -O-CH_2-CH_3 groups take less space when rotating around P-O-P bond than do the -$N(CH_3)_2$ groups.

The triplet like resonances in the ^{13}C spectra of compound **5** originate from the second order phosphorus-phosphorus coupling. The simulation of the ^{13}C resonances for compound **5** gives the correct shape only if the coupling between the magnetically non-equivalent phosphorus nuclei is larger than ±14 Hz. If a coupling constant -17.9 Hz is used, there is no visible difference between the simulated and measured resonances. The iterated ^{13}C NMR parameters are shown in Table 1, and the simulated resonances compared to the measured ones in Figure 7.

^{31}P NMR spectra chemical shift had been measured previously[13], and our results are not far from those. The ^{31}P spectrum was simulated with the final iterated parameters from ^{1}H analysis. Simulation produced visually good fit and the results are shown in Figure 7.

CONCLUSION AND PROSPECTS

A detailed NMR analysis of four biologically important pyrophosphates, was carried out. Even if the spectral parameters of all compounds are close to the published parameters of Tabun, the iteration and final results could only be achieved with taking the whole spin-systems into the calculations. Only $^{13}C\{^{1}H\}$ spectra could be solved with sub-spectral analysis because of the isotopic abundance.

One feature that this analysis showed was that there can be second order effect distributed between other than proton spin ½ nuclei. Coupling between phosphorus nuclei had effect also on the signal shapes of protons and carbons.

Unexplained fine structures in the resonance of H-c of compound **3** and C-a of compound **2** were observed. Simple torsion energy calculations did not show real evidence for torsional isomers, which could have explained the fine structures observed experimentally. Hydrogen bond formation could be another reason for the observed splitting. Further calculations and measurements in different temperatures are needed to fully explain the spectral fine structure.

During the torsion energy calculations it was seen that the P-O-P bridge did not favor a discrete geminal angle, but varied quite a lot. Sometimes it flipped over to avoid opposing tensions between the groups connected by the phosphorus nuclei. This variation might be studied even further, since there are similar -O- bridges in many organic and inorganic compounds. Especially interesting would be the question, whether the geminal angle has any noticeable effect on the couplings.

It was shown that with careful analysis and good experimental spectra it is possible to solve the population differences between stereoisomeric pairs even from severely overlapping signals. Overlapping resonances can also be identified with simulating them with parameters obtained from other analyses or even from literature.

EXPERIMENTAL

Sample preparation and spectra

The NMR samples were obtained from OPCW (Organisation for the Prohibition of Chemical Weapons) and all the measurements were made in OPCW credited Verifin laboratory in Helsinki. The samples were prepared by separately dissolving ~50 mg of **2**-**5** in 0.8 ml of $CDCl_3$ (Aldrich, 99.8 %-D). Tetramethylsilane (TMS, Sigma) served as internal chemical standard for the ^{1}H and ^{13}C spectra references. External 80 % H_3PO_4/D_2O was used for calibration of ^{31}P chemical shifts. The spectra were recorded on a Bruker AMX-400, a 400 MHz spectrometer, at +30.0 °C. The measurements were made with 5 mm QNP 1H/13C/31P/19F probe.

The 400 MHz ^{1}H NMR spectra were recorded with 32 scans, 6.6 μs pulse width (flip angle 45°), 22 s repetition time, 12.5 ppm spectral width, and 128 k points in time domain. Digital resolution in the frequency domain was 0.07 Hz/pt. The data were zero-filled and resolution enhanced by Gaussian multiplication for the iterative computer analysis.

The 100 MHz $^{13}C\{^{1}H\}$ NMR spectra were recorded with 8192 scans, 3.8 μs pulse width (flip angle 46°), 6.0 s repetition time, 250 ppm spectral width, and 64 k points in the time domain.

For the frequency domain 128 k points were used to obtain a digital resolution of 0.18 Hz/pt. Exponential multiplication was applied using a 0.5 Hz line broadening factor.

The ^{31}P and $^{31}P\{1H\}$ NMR spectra were recorded with 64 scans, 4.5 µs pulse width (flip angle 45°), 6.0-17.2 s repetition time, 163 ppm spectral width, and 64 k points in the time domain. For the frequency domain 128 k points were used to obtain a digital resolution of 0.2 Hz/pt. Exponential multiplication was applied using a 0.5 Hz line broadening factor.

Computer analysis

The 400 MHz resolution enhanced ^{1}H spectra were transferred to the PERCH[14] NMR software. After the line properties and noise had been examined, the large spectral ranges containing only noise were removed, along with all unnecessary resonances. Automatic peak picking was performed and some overlapping signals were picked with TLS (Total Line Shape) routine.

The ^{1}H NMR spectral parameters (δ_H, $^{n}J_{H,H}$) were analyzed with PERCH program by using LAOCOON and peak-top-fitting modes. The couplings from ^{31}P were solved from the splitting of each signal. Every analysis was completed with digital total line-shape fitting. The accuracy of the determined coupling constants is greater than that of parameters analyzed manually from the first order spectra.

The couplings of protons to phosphorus nuclei were confirmed with simulating the ^{31}P spectra with the chemical shifts and the coupling constants from ^{1}H analysis. Simulations of ^{31}P spectra with the ^{13}C satellites were made, but the results are not presented here. Simulated spectra with final results were compared to spectra without any extra enhancement, and visual good fitting was observed.

Table 1. The iterated NMR spectral parameters of compounds **1**-**5**. Compound **3** has two separate stereoisomeric pairs with different chemical shifts and coupling constants. The different population pairs of compound **3** are marked with **bold** or ***bold+italics*** (less abundant) when solved.

	1 (*)	**2**	**3**	**4**	**5**
$\delta_{H\text{-}a}$, J(x)	**4.271, -10.12 ($H_{a'}$), 7.07 (H_b), 9.91 (P)**	**4.130, -10.15 ($H_{a'}$), 7.09 (H_b), 7.98 (P_i)**	**4.120/4.143, -10.15/-10.12 ($H_{a'}$), 7.09 (H_b), 8.09/8.2 (P)**	**4.156, -10.15 ($H_{a'}$), 7.09 (H_b), 8.11 (P_i)**	**4.264, -10.07 ($H_{a'}$), 7.11 (H_b), 8.27 (P)**
$\delta_{H\text{-}a'}$, J(x)	**4.264, 7.06 (H_b), 8.36 (P)**	**4.089, 7.07 (H_b), 8.00 (P_i)**	**4.094/4.105, 7.09/7.10 (H_b), 7.90 (P)**	**4.134, 7.09 (H_b), 8.05 (P_i)**	**4.256, 7.04 (H_b), 8.42 (P)**
$\delta_{H\text{-}b}$, J(x)	**1.435, 0.71 (P)**	**1.354, 0.95 (P_i)**	**1.354/*1.352*, 1.01/*0.76* (P)**	**1.364, 0.99 (Pi)**	**1.387, 1.18 (P)**
$\delta_{H\text{-}c}$, J(x)	**2.783, 11.29 (P)**	**2.748, 10.89 (P_i)**	**2.742/*2.747*, 11.01/*10.97* (P)**	**4.252, -10.31 ($H_{c'}$), 7.06 (H_d),5.98 (P_{ii})**	
$\delta_{H\text{-}c'}$, J(x)				**4.248, 7.11 (H_d), 9.85 (P_{ii})**	
$\delta_{H\text{-}d}$, J(x)		**2.707, 10.64 (P_{ii})**		**1.380, 0.78 (P_{ii})**	
$\delta_{H\text{-}e}$, J(x)		**2.696, 10.58 (P_{ii})**		**4.232, -10.06 ($H_{e'}$), 7.07 (H_f), 7.06 (P_{ii})**	
$\delta_{H\text{-}e'}$, J(x)				**4.227, 7.09 (H_f), 8.86 (P_{ii})**	
$\delta_{H\text{-}f}$, J(x)				**1.379, 0.78 (P_{ii})**	
$\delta_{H\text{-}g}$, J(x)				**2.752, -10.93 (P_i)**	
$\delta_{C\text{-}a}$, J(x)	**63.90, 5.8 (P)**	**62.696, 5.21 (P_i)**	**62.865/*62.992*, 5.04/*5.27* (P)**	**63.308, 5.34 (P_i)**	**65.215, 5.98 (P)**
$\delta_{C\text{-}b}$, J(x)	**15.92, 6.8 (P)**	**16.112, 7.23 (P_i)**	**16.050/*16.070*, 7.24/*7.19* (P)**	**16.018, 7.19 (P_i)**	**16.007, 7.12 (P)**
$\delta_{C\text{-}c}$, J(x)	**35.51, 5.0 (P)**	**36.658, 4.01 (P_i)**	**36.621/*36.605*, 3.85/*3.97* (P)**	**64.855, 5.84 (P_{ii})**	
$\delta_{C\text{-}d}$, J(x)		**36.589, 4.20 (P_{ii})**		**16.057, 7.29 (P_{ii})**	
$\delta_{C\text{-}e}$, J(x)		**36.564, 4.32 (P_{ii})**		**64.81, 5.87 (P_{ii})**	
$\delta_{C\text{-}f}$, J(x)				**16.044, 7.20 (P_{ii})**	
$\delta_{C\text{-}g}$, J(x)				**36.558, 4.19 (P_i)**	
δ_{PI}	**-8.98**(+10.7***)**	**1.027, -17.91 (P_{ii})**	**0.85/0.59, -18.10 (P_{ii})**	**0.57, -17.99 (P_{ii})**	**-13.28, -16.53 (P_{ii})**
δ_{PII}		**10.970**		**-12.18**	

(*) Parameters of Tabun from Ref. 1 and Inorg. Chem. 1977, 16(11) p. 2099-2805
(**) ^{31}P chemical shift of Tabun from Anal. Chem. 69 (1997) 2694, and *** Annals New York Academy of Sciences 70, (1959) DOI: 10.1111/j.1749-6632.1958.tb35438.x

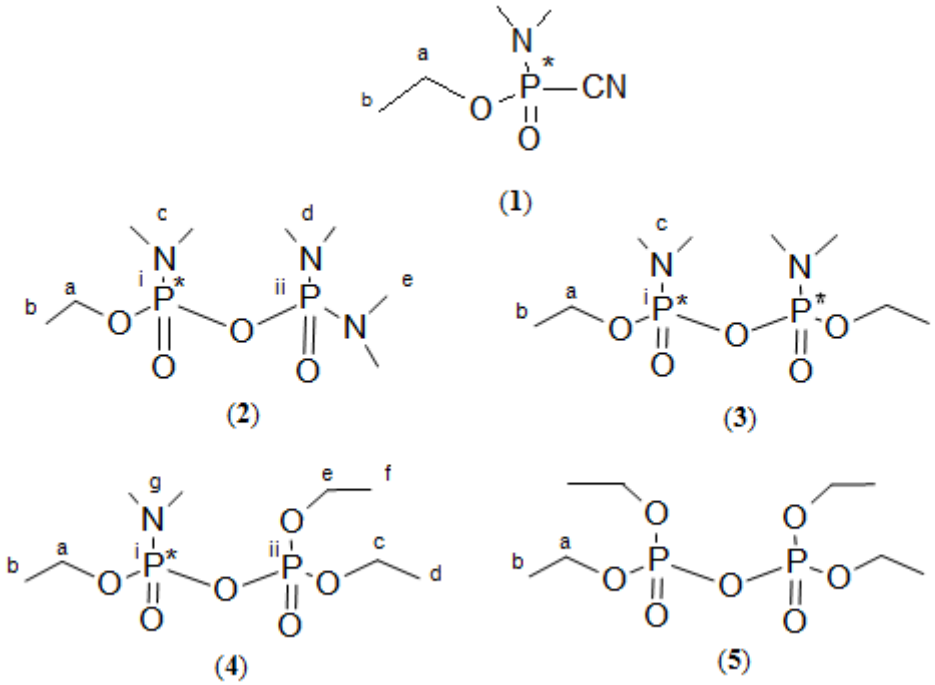

Figure 1. *O*-ethyl *N*,*N*-dimethylphosphoramidocyanidate (GB, Tabun,1), Ethyl dimethylphosphoramidic tetramethylphosphoramidic anhydride (2), Bis(ethyl dimethylphosphoramidic) anhydride (3), Diethyl phosphoric ethyl dimethylphosphoramidic anhydride (4) and Bis(diethyl phosphoric) anhydride (TEPP, 5). Asterisk marks the chiral centers in each molecular structure.

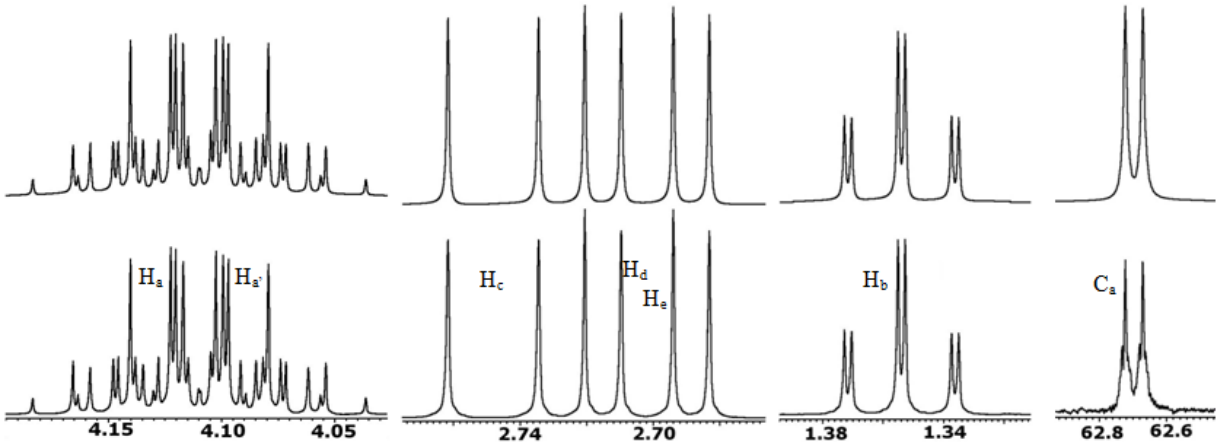

Figure 2. ^{1}H, ^{13}C-{^{1}H}, and ^{31}P spectral resonance expansions (below) of compound **2** compared to the simulated ones (above). The measured C-a resonance shows fine structure that needs further explanation. P_{ii} and P_i resonances are only simulated with parameters from ^{1}H analysis.

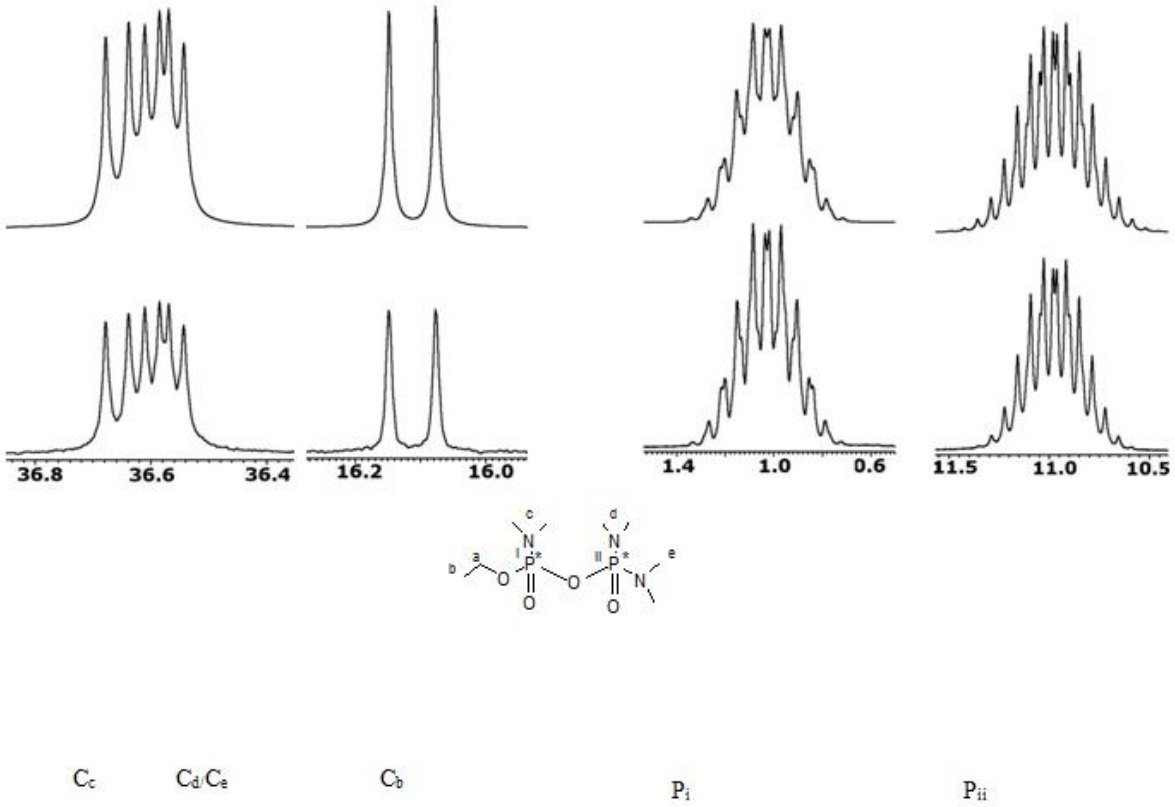

Note! The resonance intensities are not in scale.

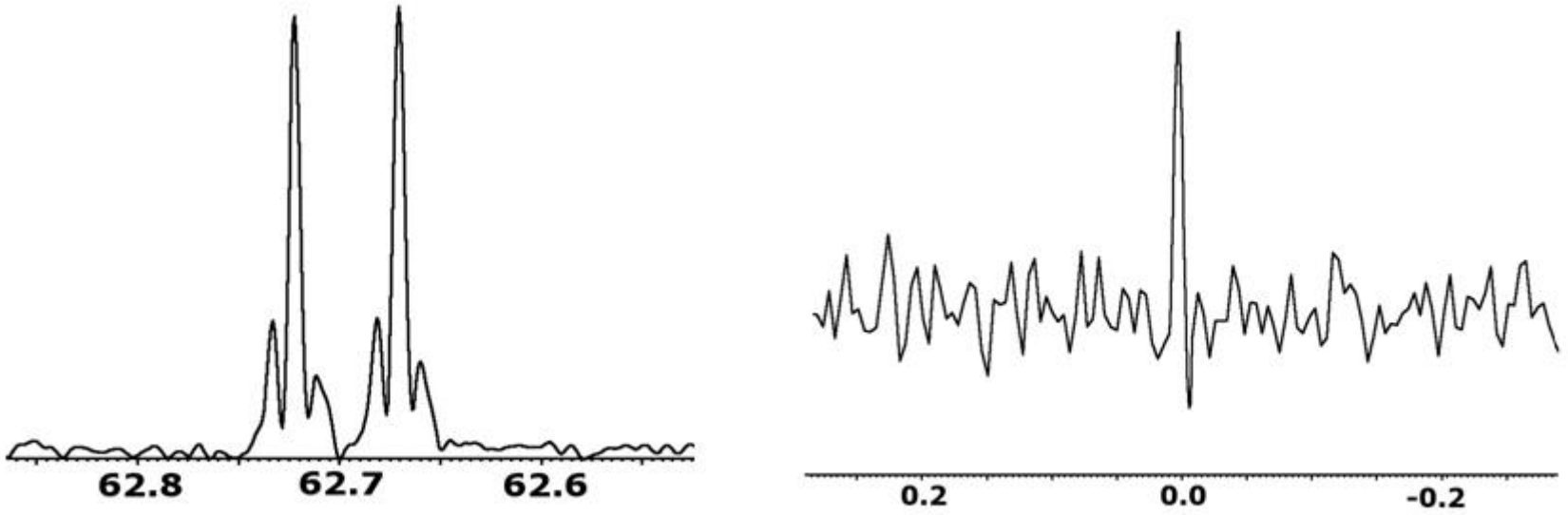

Figure 3. ^{13}C-{^{1}H} resonance signal of C-a of compound **2** after Gaussian apodization compared to TMS signal. Both of the expansions are in PPM scale. Intensities of the resonances are not in scale.

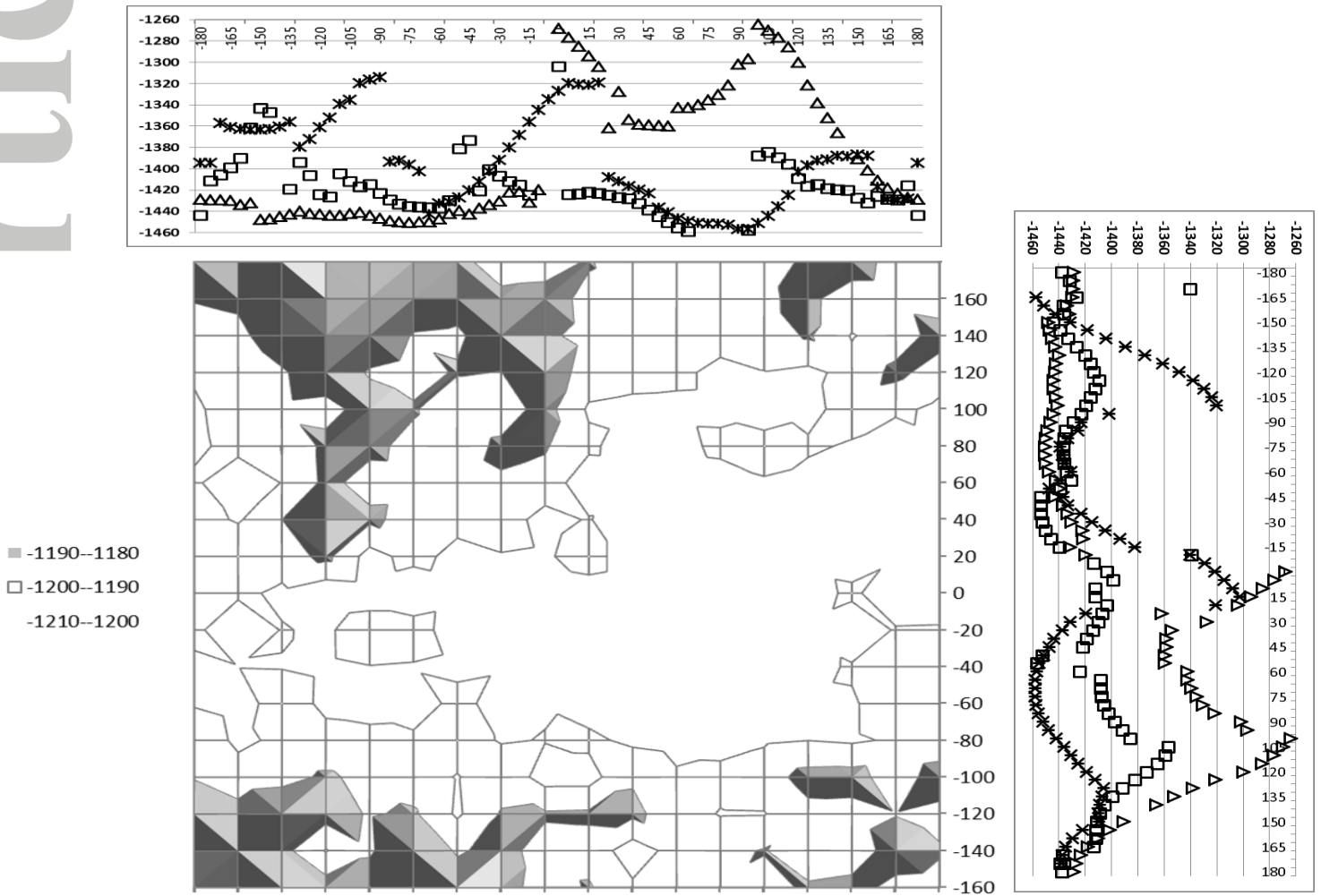

Figure 4. Torsional energy map of compound **2** over the P-O-P bridge. The 2D map is made with 20° accuracy with the PM3 method, and the slices from 120° (X), 20° (□), and -100° (Δ) in both dimensions are made with 5° accuracy using molecular mechanics method.

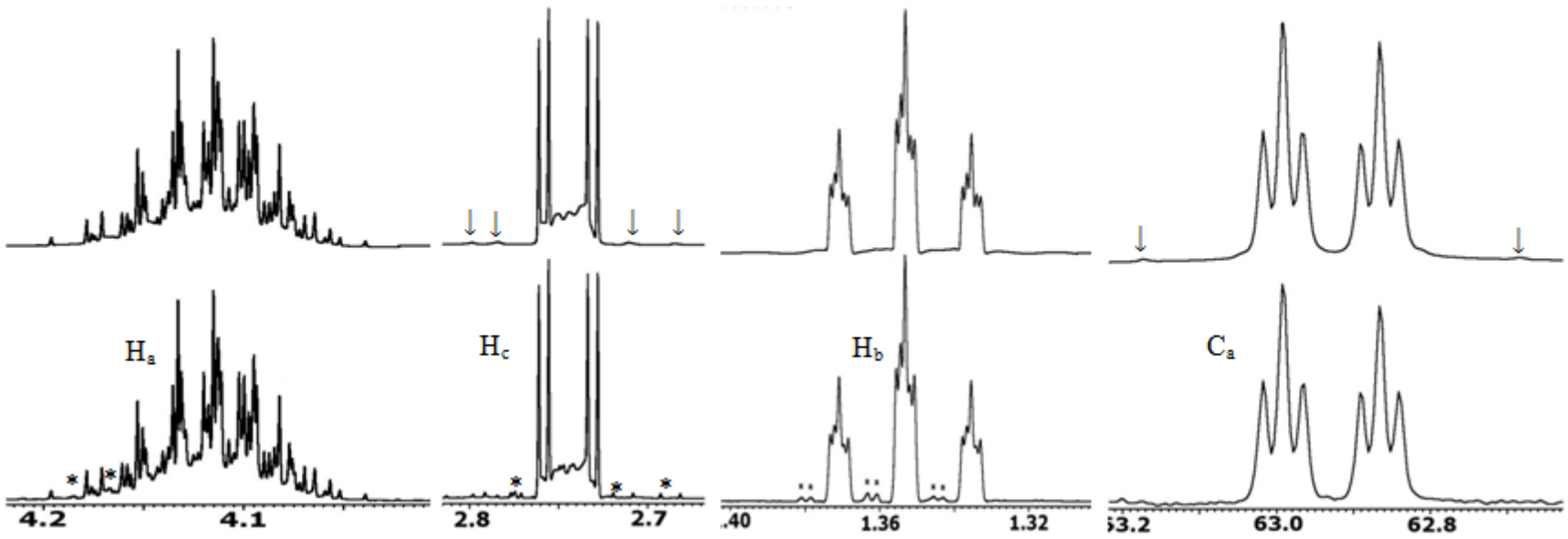

Figure 5. ^{1}H, ^{13}C-{^{1}H}, and ^{31}P spectral resonance expansions (below) of compound **3** compared to the simulated ones (above). Population differences can be seen from the intensities of the resonances. Impurity signals are marked with * and combination lines with arrows. ^{31}P spectrum is only simulated with parameters from ^{1}H analysis.

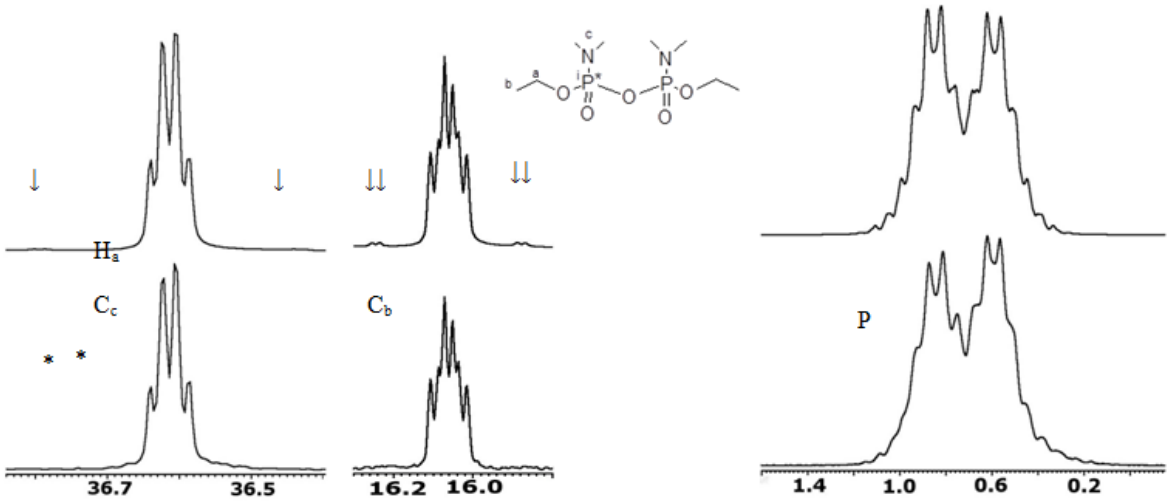

Note! The resonance intensities are not in scale.

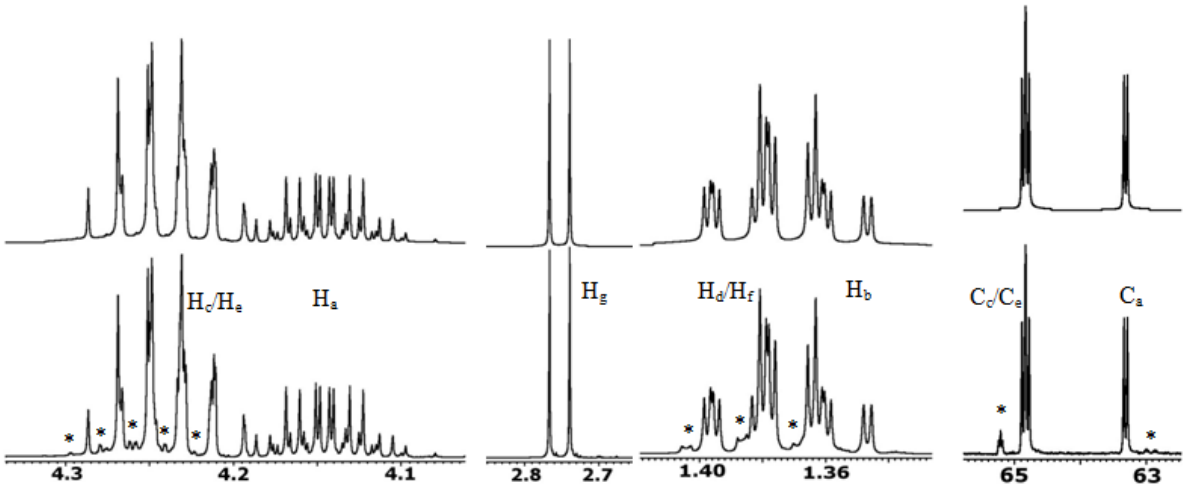

Figure 6. ^{1}H, ^{13}C-{^{1}H}, and ^{31}P spectral resonance expansions (below) of compound **4** compared to the simulated ones (above). Impurity signals are marked with *. ^{31}P resonances are only simulated with ^{1}H parameters. P_i is simulated with linewidth of 3.0 Hz and P_{ii} of 0.5 Hz.

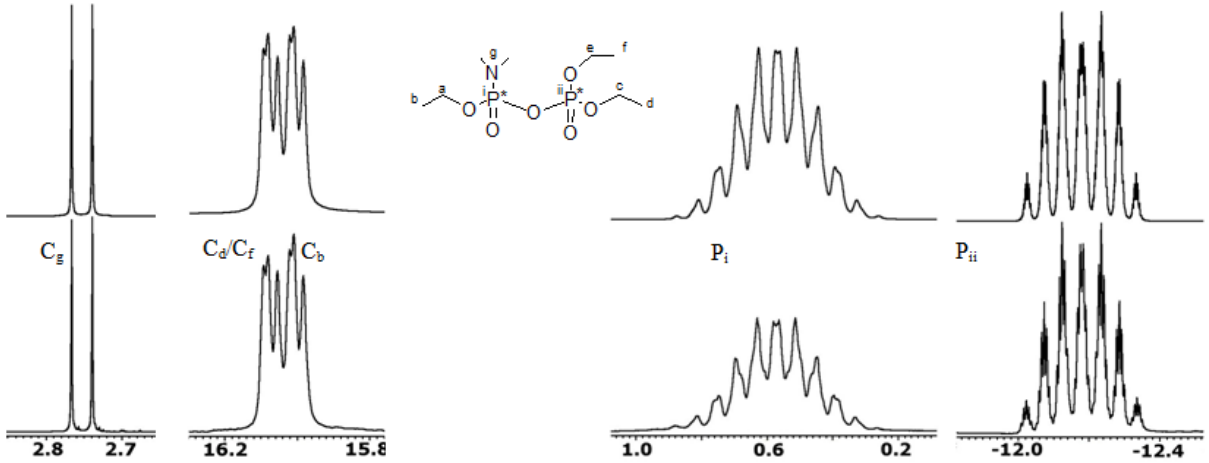

Note! The resonance intensities are not in scale.

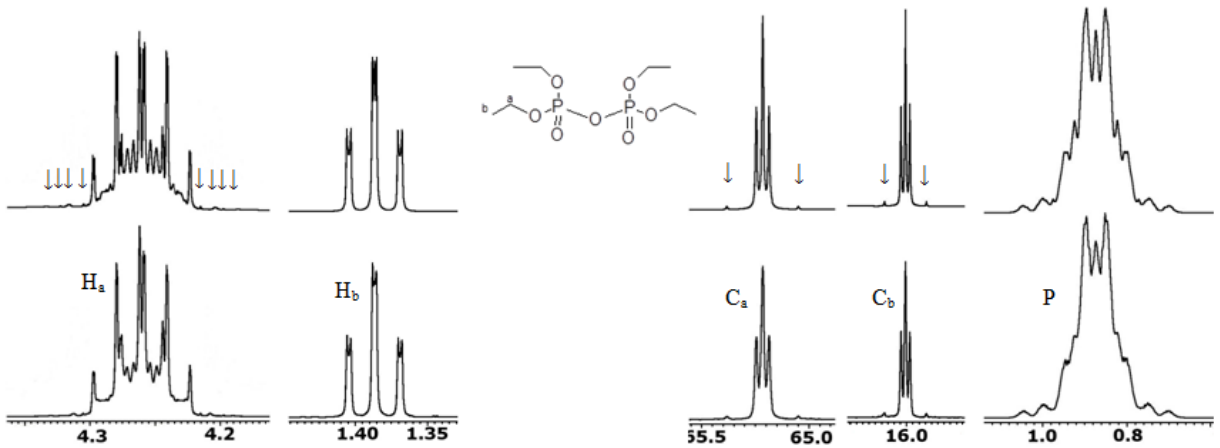

Figure 7. ^{1}H, ^{13}C-{^{1}H}, and ^{31}P spectral resonance expansions (below) of compound **5** compared to the simulated ones (above). The combination signals are marked with arrows. ^{31}P resonance is only simulated with ^{1}H parameters.

Note! The resonance intensities are not in scale.

[1] M.R. Stetten, J. Biomol. Chem., 1964, 239, 3576-3583
[2] I.R. Orriss, T.R. Arnett, R.G. Russell, Current Opinion in Pharmacology, 2016, 28, 57–68, doi:10.1016/j.coph.2016.03.003
[3] G.A. Petroianu, Die Pharmazie, 2009, 64, 269-275, doi:10.1691/ph.2009.8244
[4] C. Potter, Nature, 1949, 163, 379, doi:10.1038/163379a0
[5] M. Bothe et al. (eds.), The New Chemical Weapons Convention: Implementation and Prospects, 1998, 17-36
[6] D. J., Mowthorpe, A. C., Chapman, Spectrochimica Acta, 1967, vol.23A, 451-453, doi:10.1016/0584-8539(67)80243-5; R.K. Harris, et.al., J. Chem. Soc. A, 1967, 37-40, doi: 10.1039/J19670000037
[7] U. C. Meier, Anal. Chem., 2004, 76, 392-398, DOI: 10.1021/ac0350099
[8] C. Albaret, D. Loeillet, P. Auge´, P-L. Fortier, Anal. Chem. 1997, 69, 2694-2700, DOI: 10.1021/ac970063
[9] H. Koskela, Journal of Chromatography B, 2010, 878, 1365–1381, doi: 10.1016/j.jchromb.2009.10.030
[10] E. Vogel, U. Haberland, H.Gunther, Angew. Chem., 1970, 82, 510, doi: 10.1002/ange.19700821304
[11] Annals New York Academy of Sciences 70, (1959) DOI: 10.1111/j.1749-6632.1958.tb35438.x
[12] X. Lopez, J.I. Mujika, G. M. Blackburn, and M. Karplus, J. Phys. Chem. A 2003, 107, 2304-2315, doi: 10.1021/jp022014s
[13] R. Greenhalgh et.al. J. Agric. Food Chem., 1983, 31, 710–713, doi: 10.1021/jf00118a008
[14] R. Laatikainen, M. Tiainen, S-P. Korhonen, and M. Niemitz, Encyclopedia of Magnetic Resonance, 2011, doi: 10.1002/9780470034590.emrstm1226